Roadmap to Realistic Modeling of Closed Loop Pulsating Heat Pipes

Sameer Khandekar[§] and Manfred Groll[°]

[§] Department of Mechanical Engineering
Indian Institute of Technology Kanpur, 208016 Kanpur, India

° Visiting Professor (January 2008 - March 2008)
Indian Institute of Technology Kanpur, 208016 Kanpur, India
Consulting Engineer: 50 Panorama Street, Gerlingen, 70839, Germany

[†] corresponding author: Tel: (+91) 512 259 7038, Fax: (+91) 512 259 7408, E-mail: samkhan@iit.ac.in

Abstract

Mathematical modeling of pulsating heat pipes through 'first' principles is a contemporary problem which remains quite elusive. Simplifications and assumptions made in all the modeling approaches developed so far render them unsuitable for engineering design because the abstractions contained therein are detached from the real time transport processes taking place in the device. In this paper, a roadmap to realistic modeling scheme is presented which is based on the fact that at high enough heat flux level, Closed Loop Pulsating Heat Pipes (CLPHP) experience a bulk internal unidirectional two-phase fluid circulation; the overall internal thermo-hydrodynamic processes may be broadly seen as flow boiling/ condensation in mini-channels and conventional two-phase flow modeling may then be applied. The average two-phase flow velocity (alternatively, the net mass flux) in a CLPHP is a direct consequence of applied boundary conditions. The primary goal of any modeling strategy should therefore be to estimate the ensuing net internal two-phase mass flux, and in the process, the void fraction distribution in the loop. This indispensible information leads to the estimation of heat transfer coefficients in the evaporator/condenser sections and thus the effective thermal conductance.

With this background, a two-phase homogeneous flow model based on simultaneous conservation of mass, momentum and energy has been developed for a single loop CLPHP with all necessary boundary conditions (including the additionally necessary condition of fixed working fluid mass inventory, corresponding to the initial filling ratio of the working fluid). The closed system of equations is numerically solved, with the applicable constraint, to estimate the velocity and void fraction distribution in the loop, thereby giving the operating design curve of the single loop device and its effective thermal resistance under the applied boundary conditions. The paper also discusses the various implications of such a modeling technique.

KEY WORDS: Closed loop pulsating heat pipe, flow modeling, parametric influences.

1 INTRODUCTION

The applicable two-phase flow velocity scale and ensuing void fraction distribution in a Closed Loop Pulsating Heat Pipe (CLPHP) are not known a priori; these depend on external thermo-mechanical boundary conditions under which the device operates. The estimation of this velocity scale, given the device control parameters and operating conditions, remains the singular challenge to further progress in system modeling. Once this two-phase velocity scale is deciphered, then, although the estimation of heat transfer as a function of this scale still remains a daunting task, nevertheless, in principle, the mathematical description of the system will be complete.

Till date, modeling of PHPs has been attempted with different simplified schemes and approaches, which include [1-3]:

Type I: comparing PHP action to an equivalent single spring-mass-damper system.

Type II: kinematic analysis by comparison with a multiple spring-mass-damper system.

Type III: applying conservation equations to specified slug-plug control volume.

Type IV: analysis highlighting the existence of chaos for some operating conditions.

Type V: Artificial Neural Networks modeling.

Type VI: semi-empirical modeling by non-dimensional groups.

These modeling approaches, excepting the last, have very limited applicability as they do not represent real operational thermo-fluidic behavior. The last approach is promising, the success being limited by the complete and correct identification of all possible combinations of applicable force fields and their relative importance. In actual operation, thermally driven self-excited two-phase flow oscillations commence, resulting in different flow patterns (thus, heat transfer mechanisms), based on the applied boundary conditions. In this paper we focus our attention on modeling the CLPHP from first principles taking into account experimental evidences obtained thus far.

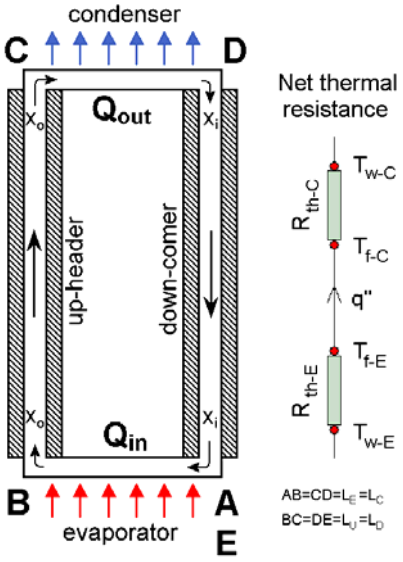

Figure 1: Schematic of the single loop pulsating heat pipe showing salient sections of the loop and the net thermal resistance.

For improving the understanding of the CLPHP operation, experimental studies have been performed in the past on the primary building block of a CLPHP, i.e. a single-loop device, as shown in Figure 1 [4-5]. A very strong thermo-hydrodynamic coupling was reported with the performance (thermal resistance) decisively linked with the flow patterns existing inside. At low heat fluxes, the two-phase fluid oscillates arbitrarily with capillary slug flow as the dominant flow pattern. With increasing input heat flux to the evaporator, the working fluid tends to take up a fixed flow direction. After a particular heat flux level to the system, the two-phase fluid flow inside the tube definitely takes up a fixed flow direction. When this happens, there are usually intermittent/ semi-annular/ annular flow conditions which exist in the upheader and bubbly or slug flow is seen in the downcomer. Under such a quasi-steady bulk flow circulation situation, the static pressure distribution, going once across the loop, should match at points A and E. Such a flow behavior is also reported by many other investigators (for example, refer [6-9]).

There is a need, as a first step, to develop a generalized model capable of predicting the average bulk two-phase flow parameters in the CLPHP under such unidirectional flow conditions, discussed above. As a next step then, pulsations on the mean flow can be superimposed to refine the model. In order to initiate this process, we need to see the processes in a CLPHP from the point of view of flow boiling/ condensation in mini-channels so as to get, at the least, a first realistic order of estimation of the velocity scales of the CLPHP system dynamics. These devices are 'closed flow' systems. In major contrast to 'open flows' in mini-channels, the inlet conditions/ parameters (for example, mass flux, vapor quality, pressure and level of subcooling) to the evaporator and condenser U-turns are not externally controllable in case of CLPHPs. These quantities depend on thermo-mechanical boundary conditions imposed on the system [10]. This paper attempts to develop the above line of thinking and propose design curves for a single loop pulsating heat pipe by simultaneously solving the mass, momentum and energy equation for a single loop pulsating heat pipe. We thus obtain the effective thermal resistance of the device.

2 WHAT DRIVES A CLPHP?

The available experimental results and trends indicate that any attempt to mathematically analyze CLPHPs must address two strongly interdependent and vital aspects simultaneously, viz. system 'thermo' and 'hydrodynamics' [11]. Figure 2 shows the genealogy of closed passive two-phase heat transfer systems. While the 'family tree' is certainly not exhaustive, most relevant systems for the present discussion are included. As will be evident shortly, although all systems shown in Figure 2 have 'similar' working principles, there are decisive differences that significantly alter the course of mathematical analyses.

Presence of a capillary wick for the fluid transport is the fundamental characteristic of the first group (Group A), consisting of conventional and loop heat pipes. While the former has counter-current flow of the two phases, it is avoided in the latter design. For analysis of such systems leading to the determination of maximum heat transport based on the capillary limit (neglecting pressure drops associated with phase change), we use the standard formulation [3]:

$$(\Delta P)_{cap} \pm (\Delta P)_{gra} \geq (\Delta P)_l + (\Delta P)_g + (\Delta P)_{l/g} \qquad (1)$$

where,

$$(\Delta P)_{gra} = (L_l^{eff} \cdot \rho_l \cdot g \cdot \sin\beta) - (L_g^{eff} \cdot \rho_g \cdot g \cdot \sin\beta) \qquad (2)$$

The R.H.S. of Eq. (1) contains 'dissipative' terms that are always numerically positive while the L.H.S. contains the 'driving' terms that must be at least equal to the R.H.S. to keep the system running[1]. Thus, all the devices in this group can function in anti-gravity mode (negative sign of $(\Delta P)_{gra}$ in Eq. (1)) if the capillary pumping is greater than the gravitational head. The inter-phase shear interaction represented by $(\Delta P)_{l/g}$ is nullified in loop heat pipes by the geometrical construction of the device rendering it to be a better alternative to conventional designs.

[1] The liquid-vapor phase interaction term $(\Delta P)_{l/g}$ is added separately here for clarity, as is usually done in heat pipe literature; if we solve the complete momentum equation with interfacial shear terms and an appropriate boundary condition at the liquid/vapor interface, its effect is implicitly included.

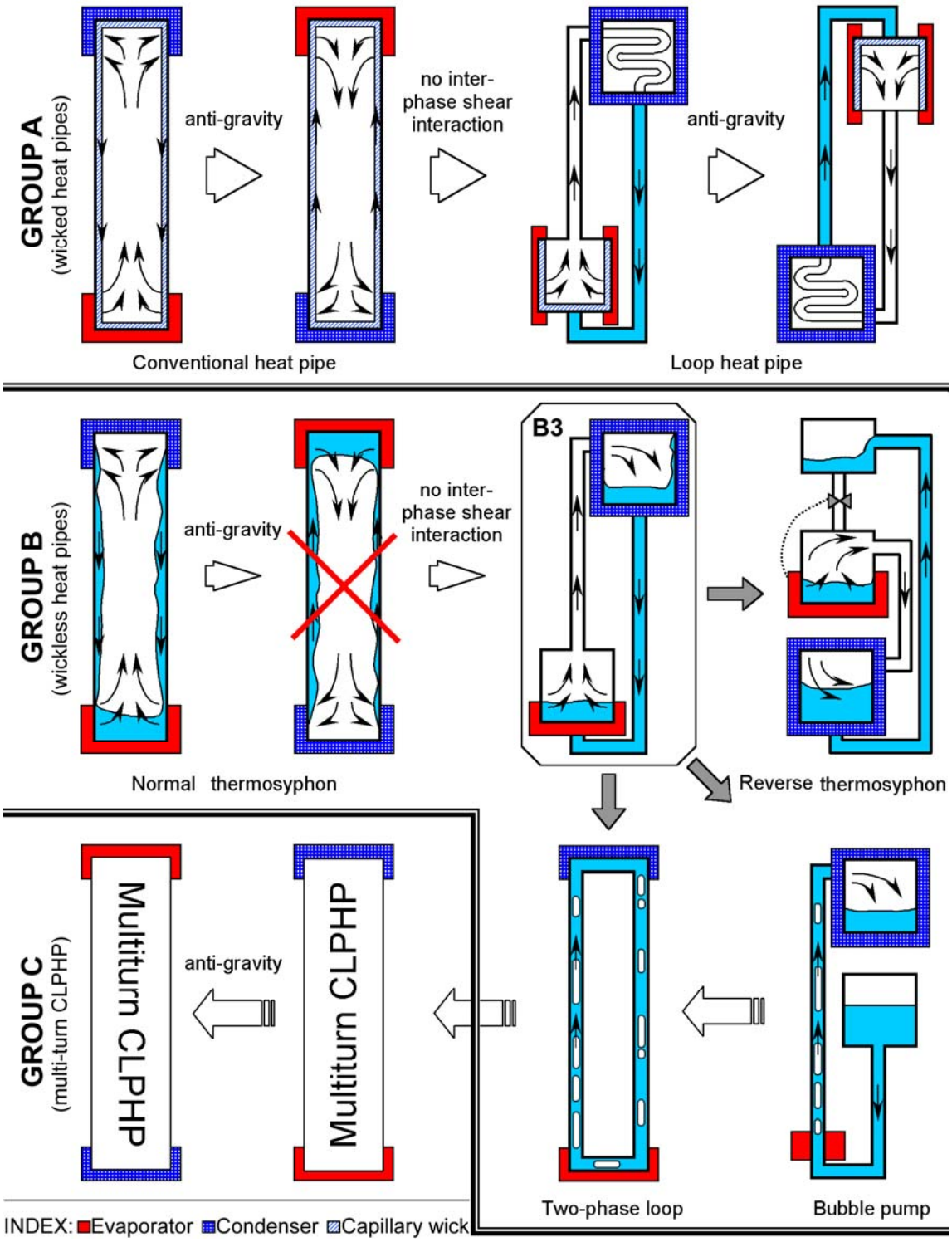

Figure 2: Genealogy of closed passive two-phase systems showing the evolution of multiturn pulsating heat pipes. Although all the systems shown above have 'similar' working principles, there are decisive differences that significantly alter the course of mathematical analyses.

If the capillary pumping of the first group of devices is made to vanish, we obtain the second group (Group B). This is represented by the gravity-assisted thermosyphons. Here, the design equation reduces to,

$$(\Delta P)_{gra} \geq (\Delta P)_l + (\Delta P)_g + (\Delta P)_{l/g} \quad (3)$$

Thus, in this group, only the gravity head provides the driving potential. Quite naturally, since the L.H.S. of Eq. (3) must always be positive for a viable system, anti-gravity (or zero gravity) operation is not feasible. Usually, $(\Delta P)_{l/g}$ limits the operation and leads to Counter-Current Flow Limitation (CCFL) [12, 13]. Such failures can be avoided in design B3 (so called, separate-type heat pipe in the common literature), where the two phases flow in separate channels. This design represents a genealogical crossroad that will lead us to Group C devices including CLPHPs. It is to be noted that all the designs discussed so far were primarily based on latent heat transfer. Although finite but small sensible heating/cooling does take place, an assumed near isothermal (or isobaric) condition within the system necessarily nullifies its impact. This assumption generally is quite realistic for devices in Group A and B.

One variation of design B3 can be done by reducing the size of the fluid transport channels and the evaporator, to capillary dimensions. One common example of such a case is the standard bubble pump in which, instead of single-phase vapor flow from the evaporator to the condenser, flow of two-phase mixture results as a direct consequence of slug flow regime being established in the upheader due to the dominance of surface tension. If the evaporator and condenser sections are joined by a capillary sized tube, this results in a capillary two-phase loop, as shown in Figure 2. The construction of these devices forces a combination of sensible as well as latent heat transfer. This marks the first significant shift from the previously discussed cases (Group A and B). The second critical aspect is that the gravity head and the dissipative terms are no more based on single-phase flown calculations but are governed by two-phase flow calculations. In addition, based on the size of the capillary tubes being used, some capillary forces may also have to be accounted for depending on their order as compared to other applicable pressure heads. What complicates the situation further is the inherent presence of two-phase flow instabilities in such systems.

Another variation of design B3 comes in the form of an anti-gravity reverse thermosyphon by incorporating a suitable remote-operated valve [14, 15]. Since there is neither capillary pumping nor positive gravity head (condenser is below the evaporator), the driving potential must come from elsewhere. At the commencement of liquid heating in the evaporator chamber, the remote-operated valve is kept closed. Boiling proceeds under nearly constant volume conditions (since there is always some liquid present in the condenser) thereby increasing local vapor pressure and temperature. After a while, the evaporator pressure becomes high enough to push liquid out of the condenser, against gravity, towards the accumulator. The evaporator gradually empties while the accumulator starts filling up. A stage comes when all the evaporator liquid is boiled off. This stage is immediately followed by a rise in heater temperature and a drop in evaporator chamber pressure as the remaining vapor also condenses. The valve is now triggered to open by either of these signals, creating pressure equalization between the accumulator and evaporator by gravity assisted liquid return. The cycle then repeats itself. Thus, we observe that a slight design variation necessitates a change in the driving potential; the applicable design criterion now becomes,

$$(\Delta P)_{sat}^{E-Acc} - (\Delta P)_{gra} \geq (\Delta P)_l + (\Delta P)_g \quad (4)$$

where,

$$(\Delta P)_{sat}^{E-Acc} = (P)_{sat}\big|_E - (P)_{sat}\big|_{Acc} \quad (5)$$

and,

$$(\Delta P)_{gra} = (L_l^{eff} \cdot \rho_l \cdot g \cdot \sin\beta) - (L_g^{eff} \cdot \rho_g \cdot g \cdot \sin\beta) \quad (6)$$

With the preceding discussion we conclude that the 'driving' terms in the entire family of these passive two-phase heat transfer devices are $(\Delta P)_{gra}$, $(\Delta P)_{cap}$ or $(\Delta P)_{sat}$, acting individually or in combinations, as per the case.

2.1 Governing equation for CLPHP

The most complicated situation will arise if all the 'driving' terms, discussed above, are simultaneously present and the two phases are not flowing separately but as a mixture; the design equation then takes the following form (again neglecting the pressure drops associated with phase change in the evaporator and the condenser):

$$\sum_1^2 (\Delta P)_{cap} + \sum_1^2 (\Delta P)_{sat} \pm \sum_1^2 (\Delta P)_{gra}^{two-phase} \geq \sum_1^2 (\Delta P)_{two-phase} \quad (7)$$

where 1 and 2 are specified locations in the system. The R.H.S. includes dissipation due to two-phase friction and acceleration components.

A multiturn CLPHP is a thermo-hydrodynamic genesis of a reverse thermosyphon (without control valve!), a bubble pump and a two-phase loop and hence represents the most complicated case. Coming to the simplistic case of a single-loop PHP, we can argue that it operates only due to the mixture density difference in the two arms, upheader and downcomer, which in turn changes the gravitational head in the two sections. This positive driving gravitational potential head must overcome the frictional and acceleration head due to the two-phase flow for the loop to operate satisfactorily. While this argument is correct for a single loop device, a multi-turn PHP also works

very satisfactorily in anti-gravity top heater mode [16-19]. In such a situation, gravity does not support the fluid movement but is, in fact, opposing it. Thus, there must be an additional driving potential available inside the system to overcome the dissipation due to friction, acceleration and gravitational pressure drops i.e. $\sim(\Delta P)_{sat}^{dyn}$. This force is rendered by bubble pumping/collapsing action and it becomes predominant as the number of turns increase beyond a particular critical number. The magnitude is affected by the dynamic forces associated with rapid bubble growth and collapse in various sections of the CLPHP tube. Fast bubble growth and collapse leads to forces due to rapid momentum change of the vapor phase which can attain comparable values to other interacting forces like surface tension, inertia forces, gravity force and viscous forces. In addition, rapidly pulsating flows also get affected by various forms of two-phase flow instabilities and possible metastable conditions. Even if $(\Delta P)_{cap}$ is assumed to be negligible (which is generally true for the channel diameters as applicable for CLPHPs), given the fact that anti-gravity operation of multiturn CLPHPs is indeed possible, some form of effective $(\Delta P)_{sat}^{dyn}$ must invariably operate due to generation and collapse of bubbles, as discussed before, so as to provide a net positive driving potential. Modeling of this spatially and temporally varying term is the most challenging task and is yet to be achieved. It is to be noted that Eq. (7) governs one of the most important operational limits of the pulsating heat pipes. Analogous to conventional heat pipes, several other physical situations may also arise leading to other operational limits, e.g. the boiling limit and some form of two-phase sonic limit, which we shall not discuss here.

For the case of a single-loop PHP considered in this study, experimental studies show that it does not work in horizontal or anti-gravity orientation [1-5]. It is obvious therefore that $(\Delta P)_{gra}^{two-phase}$ is the main dominant driving force. Thus, in this study, we will explore the applicability of the following design equation for a single-loop PHP, working under the action of gravity assistance only:

$$\sum_{E}^{C}(\Delta P)_{gra}^{two-phase} = \sum_{E}^{C}(\Delta P)_{two-phase} \tag{8}$$

It should be noted that Eq. (7) or (8) is in essence, a coupled momentum and energy equation. This is because the RHS (dissipative two-phase friction and acceleration terms) and the LHS (driving gravitation terms) are both affected by the thermal energy input and output boundary conditions. While proposing Eq. (8) as the design equation of the single loop device, we neglect $(\Delta P)_{sat}^{dyn}$ and $(\Delta P)_{cap}$. As will be explained in the next section, Eq. (8) is a necessary but not a sufficient condition for a PHP.

2.2 Mass inventory or void fraction constraint

A CLPHP is a 'closed flow' device and thus the mass inventory which goes inside the device at the time of filling remains constant throughout its operation. Thus, for a closed flow system as represented by Figure 1, an additional constraint on Eq. (8) when applied to a closed loop system is:

$$\bar{m}_{ini} = \frac{1}{L_{total}} \oint_{A-E} m \cdot dz = \text{constant} \tag{9}$$

Therefore, at all operation times, the fluid mass inventory, spatially integrated over the closed loop, must remain constant whatever be the external boundary conditions applied on the loop.

If we assume that the temperature variation while operation is small then the respective phase density variations can be neglected i.e. fog flow model is valid. Then, we can also write Eq. (9) as:

$$\bar{\alpha}_{ini} = \frac{1}{L_{total}} \oint_{A-E} \alpha \cdot dz = \text{constant} \tag{10}$$

The average void fraction, found by integrating the local void fraction over the entire closed loop, must also remain constant at all times whatever be the external boundary conditions applied on the loop. In other words, for homogeneous flow assumptions, conservation of total mass inventory is practically the same as conservation of the total volume of the pseudo homogeneous fluid [10].

Figure 3 depicts the variation of liquid filling ratio with respect to the operating temperature for working fluids water and ethanol. This means that if we fill in the pulsating heat pipe by say 50% liquid at room temperature (25°C) and then the loop operates at a mean temperature of say, 100°C, then the effective mean FR integrated over the entire loop at 100°C would be somewhat less than 50%. The decrease takes place because of the change in the respective mean specific volumes of the two phases with respect to the temperature. As can be seen in Figure 3, the change in effective filling ratio with operating temperature is less for water than for ethanol. Therefore, the ensuing inaccuracy by the use of Eq. (10) instead of Eq. (9) would be less in case of water than for ethanol. In general, provided the temperature dependency of the filling ratio is accounted/corrected for, Eq. (10) is more convenient to use than Eq. (9) as it deals with a non-dimensional quantity ($\bar{\alpha}_{ini}$ or (1-FR)).

The void fraction constraint, as discussed above, has far reaching consequences on the operation of CLPHPs. For example, if the initial filling ratio is, say 80%, i.e., $\bar{\alpha}_{ini} = 0.2$, it is extremely unlikely that churn or fully annular flow ever develops. Any increase in void fraction in the evaporator and upheader must be associated with a

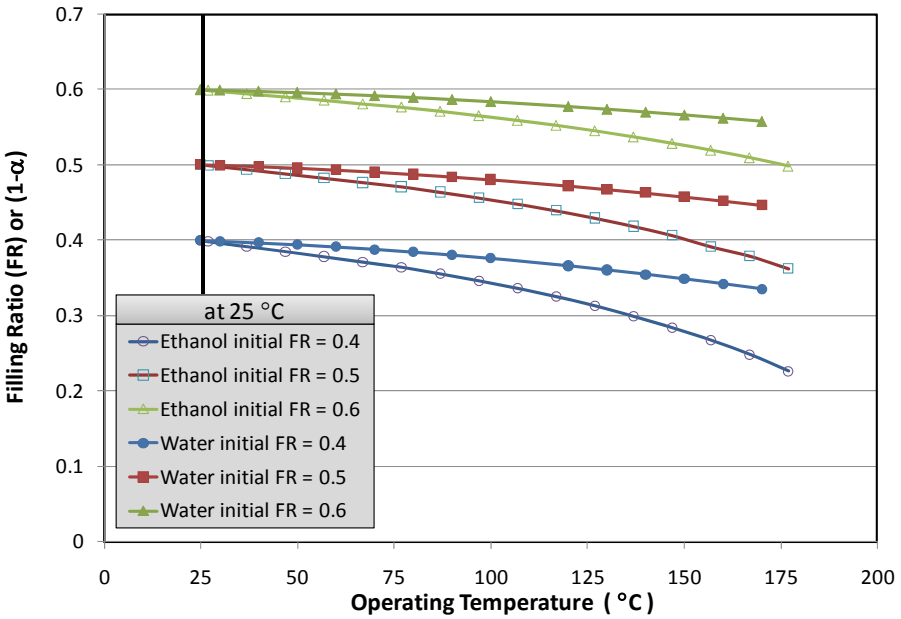

Figure 3: The variation of liquid Filling Ratio (V_l/V_{tot}) of the closed loop pulsating heat pipe with its operating temperature is depicted in this figure. Initial liquid filling ratio is specified at 25°C. As the operating temperature of the PHP increases, the original FR, based on 25°C room temperature, changes. For water the variation is not as high as for ethanol.

subsequent decrease in void fraction elsewhere in the system. Thus, there exists a dynamic feedback mechanism inside the loop which is active at all times forcing the constraint given by Eq. (9) to be fulfilled for the loop. For real time processes the feedback-correction loop will require finite time. And therefore to satisfy Eq. (9) or (10), metastable conditions will be inherent to the system dynamics. With the above arguments we conclude that for predefined and fixed external boundary conditions, the simultaneous solution of Eq. (8) (combined momentum and energy conservation) and Eq. (9) (or Eq. 10, conservation of total void fraction) is essential to get the complete design equation of the single loop two-phase device.

3 MODEL DESCRIPTION

We now formulate the model for a closed single loop device as shown in Figure 1, representing Eq. (8) and Eq. (9). Before we proceed, we list the major assumptions in this formulation.

- Homogeneous fog-flow conditions exist; the relation between the vapor mass fraction and void fraction is given by:

$$\frac{x}{(1-x)} = \frac{\alpha}{(1-\alpha)} \frac{\rho_g}{\rho_l} K \qquad (11)$$

  where the slip ratio $K = 1$ for homogeneous flow.
- Flashing/phase-compressibility is neglected.
- Both phases are in thermodynamic equilibrium.
- Constant heat flux boundary conditions exist in the evaporator and condenser sections.
- Upheader/ downcomer sections are adiabatic.
- Thermo physical properties of the working fluid are taken at the mean operating temperature (defined as $(T_E+T_C)/2$).
- The mean viscosity of the fluid is given by the Cicchitti [20] model:

$$\mu_m = x\mu_g + (1-x)\mu_l \qquad (12)$$

- The flow is assumed to be turbulent everywhere so the value of C_f is given by $C_f = 0.079\mathrm{Re}^{-1/4}$ (where $\mathrm{Re} = GD/\mu_m$). Although C_f varies along respective sections of the loop because of the applied boundary conditions, for simplicity, it is assumed to be constant while integrating the set of equations.
- Additional pressure drop in the tube bends is neglected.

The implications of the above assumptions are summarized in Table 1.

Referring to Table 2, the generalized pressure gradient in the individual tube sections of the closed loop device is given by Eq. (13). Incorporating the assumptions outlined above, the value of pressure drop in the respective sections of the closed loop device, i.e. $(\Delta P)_E$, $(\Delta P)_U$, $(\Delta P)_C$ and $(\Delta P)_D$ are given by Eqs. (14) - (17) in Table 2. Since the pressure drop across the loop has to be zero, the governing equation of the loop is given by Eq. (18). Substituting the values of individual pressure drops in respective loop sections we get the combined applicable governing equation for the loop i.e. Eq. (19) in Table 2. This is the principal governing equation for the closed single loop PHP for the calculation of mass flux (G) through the system for a given boundary condition.

Table 1: Conditions existing in various sub-sections of the closed loop

	Evaporator	**Upheader**	**Condenser**	**Downcomer**
Enthalpy	$\frac{d\hat{h}}{dz}=\frac{4q''}{GD}$	0	$\frac{d\hat{h}}{dz}=-\frac{4q''}{GD}$	0
Dryness fraction	$x=x_i+\frac{4q''z}{GDh_{fg}}$ $x=x_i$ at entry $x=x_0$ at exit	$x=x_o$ $x=x_0$ for all L_U	$x=x_o-\frac{4q''z}{GDh_{fg}}$ $x=x_0$ at entry $x=x_i$ at exit	$x=x_i$ $x=x_i$ for all L_D
Length	$L=L_E=L_C$	$\bar{L}=L_U=L_D$	$L=L_C=L_E$	$\bar{L}=L_D=L_U$
Angle with horizontal	0°	90°	0°	-90°
Void fraction	$\alpha_E=\left[(1-\frac{\rho_g}{\rho_l})+\frac{\rho_g/\rho_l}{\left(x_i+\frac{4q''z}{GDh_{fg}}\right)}\right]^{-1}$	$\alpha_U=\left[(1-\frac{\rho_g}{\rho_l})+\frac{\rho_g/\rho_l}{(x_o)}\right]^{-1}$	$\alpha_C=\left[(1-\frac{\rho_g}{\rho_l})+\frac{\rho_g/\rho_l}{\left(x_o-\frac{4q''z}{GDh_{fg}}\right)}\right]^{-1}$	$\alpha_D=\left[(1-\frac{\rho_g}{\rho_l})+\frac{\rho_g/\rho_l}{(x_i)}\right]^{-1}$
Constant C_f calculated on the basis of	$x=\bar{x}=(x_i+x_o)/2$	$x=x_o$	$x=\bar{x}=(x_i+x_o)/2$	$x=x_i$

Table 2: List of equations appearing in the model

Item	#	**Expression**
General equation	(13)	$\left(\frac{dP}{dz}\right)=\frac{2C_fG^2}{D}\left[xv_g+(1-x)v_l\right]+\frac{G^2}{h_{fg}}\frac{d\hat{h}}{dz}\left(v_g-v_l\right)+\rho g\sin\beta$
Evaporator	(14)	$\left(\Delta P\right)_E=G^2\left[\frac{2C_fL}{D}\left\{x_iv_g+\left(1-x_i\right)v_l\right\}\right]+G\left[\frac{4C_fq''L^2}{D^2h_{fg}}\left(v_g-v_l\right)+\frac{4q''L}{Dh_{fg}}\left(v_g-v_l\right)\right]$
Up header	(15)	$\left(\Delta P\right)_U=G^2\left[\frac{2C_f\bar{L}}{D}\left\{x_ov_g+\left(1-x_o\right)v_l\right\}\right]+\frac{g\bar{L}}{\left\{x_ov_g+(1-x_o)v_l\right\}}$
Condenser	(16)	$\left(\Delta P\right)_C=G^2\left[\frac{2C_fL}{D}\left\{x_ov_g+\left(1-x_o\right)v_l\right\}\right]-G\left[\frac{4C_fq''L^2}{D^2h_{fg}}\left(v_g-v_l\right)+\frac{4q''L}{Dh_{fg}}\left(v_g-v_l\right)\right]$
Down comer	(17)	$\left(\Delta P\right)_D=G^2\left[\frac{2C_f\bar{L}}{D}\left\{x_iv_g+\left(1-x_i\right)v_l\right\}\right]-\frac{g\bar{L}}{\left\{x_iv_g+(1-x_i)v_l\right\}}$
Governing equation for the Loop	(18)	$\left(\Delta P\right)_E+\left(\Delta P\right)_U+\left(\Delta P\right)_C+\left(\Delta P\right)_D=0$
Combined final equation	(19)	$G^2\left[\frac{2C_f\left(L+\bar{L}\right)}{D}\left\{\left(v_g-v_l\right)\left(x_o+x_i\right)+2v_l\right\}\right]+\frac{g\bar{L}}{\left\{x_ov_g+\left(1-x_o\right)v_l\right\}}-\frac{g\bar{L}}{\left\{x_iv_g+\left(1-x_i\right)v_l\right\}}=0$
Note: $L=L_E=L_C$ and $\bar{L}=L_U=L_D$		

As can be appreciated, the loop is driven by the density difference in the upheader and the downcomer (second and third terms of Eq. 19). This driving force must overcome the frictional two-phase pressure drop represented by the first term of Eq. (19). Apart from this equation, for a closed loop device to operate, it must also satisfy the total mass inventory constraint, as discussed earlier in Section 2.2.

4 SOLUTION PROCEDURE

The geometrical parameters of the loop are first fixed, i.e. internal diameter D and length of respective sub-sections, L_E, L_C, L_U and L_D. The steady state combined momentum and energy equation of the closed loop represented by Eq. (19) (derived from Eq. (8)) is then solved for a given value of heat input and assumed operating temperature of the loop. The thermophysical properties of the working fluid correspond to the assumed operating temperature. The vapor mass fraction changes in the evaporator (from x_i to x_o) and condenser sections (from x_o to x_i) but remains fixed in two adiabatic sections (x_o in Upheader and x_i in Downcomer). An initial guess for x_i (in the downcomer, entry to the evaporator) and loop mass flux *G* is needed so as to estimate the coefficient of fog-flow friction i.e. C_f. The value of x_o is then calculated as per Table 1 and the simulation is initiated. An iterative shooting technique is adopted to estimate and update the value of the mass flux *G*, which finally converges and satisfies Eq. (19). Thus, for a given heat input, depending on the operating temperature, the interplay of the buoyancy force difference created in the upheader and downcomer due to heating and cooling process, and the frictional shear stress in the loop due to the ensuing flow, provides a unique value of mass flux *G* from Eq. (19). Now, as we have noted earlier, the loop must satisfy the total mass inventory constraint also, i.e. Eq. (8), depending on the initial filling ratio of the working fluid. Based on the homogeneous flow assumption, solution of Eq. (19) also provides the mean density distribution or the mean void fraction distribution in the loop (refer Eq. (11)). With this information, the total mass inventory (or alternatively, the average void fraction, as discussed above) can then be found.

5 RESULTS AND DISCUSSION

5.1 Design curve of single loop device

The above solution procedure is repeated for different heat inputs and plotted in Figure 4 (a) for ethanol, (b) for water. The geometrical parameters for which these simulations have been carried out are noted on the figure. Heat input to the loop is varied from 10 W-50 W (q″=2.1-10.6 W/cm^2). The solid lines represent the solution of Eq. (9). The domain of the curve will lie between the freezing temperature and the critical temperature of the working fluid. As we approach near these limits, the mass flux will obviously fall to zero. The cross lines represent the constant mass inventory or constant void fraction (iso-void) lines corrected for temperature with reference to Figure 3. These represent the loci of points on which Eqs. (8) and (9) are simultaneously satisfied. During operation, as can be seen, depending on its initial fill charge/ mass inventory, the loop will follow a particular iso-void line. Taking an example of a water filled device with FR = 55% at 25°C we note that as the heat input increases from 10 W to 50 W there is, in fact, a slight reduction in the net mass flux in the loop. The operating temperature increases from about 120°C to 162°C (the thermophysical properties need to be updated with changing operating temperature). While the increased heat input increases the density difference in the upheader and the downcomer, this increased gravitational operating potential is compensated by increase of two-phase frictional resistance.

5.2 Effective thermal resistance

Once the design curve is constructed, as outlined above, the effective thermal resistance of the loop can be estimated. Referring to Figure 5, at any operating temperature, as the two-phase mass flux and the spatial void distribution is known, we can estimate the thermal resistance in the evaporator and condenser sections. The net thermal resistance is a linear combination of these two constituent elements, as shown in the figure.

For calculating the heat transfer coefficient in the evaporator tube section we use the Kandlikar correlation along with the applicable constants C_1 through C_4 given by [20]:

$$h_E = h_{lo}\left[C_1 \underline{\mathrm{Co}}^{C_2} + C_3 \underline{\mathrm{Bo}}^{C_4}\right] \tag{20}$$

where,

$$h_{lo} = 0.023 \cdot \left(\frac{k_l}{D}\right) \mathrm{Re}_l^{0.8}\, \mathrm{Pr}_l^{0.4} \tag{21}$$

$$\underline{\mathrm{Co}} = \left(\frac{1-\overline{x}}{\overline{x}}\right)^{0.8} \left(\frac{\rho_g}{\rho_l}\right)^{0.5} \tag{22}$$

$$\underline{\mathrm{Bo}} = \left(\frac{q''}{G \cdot h_{fg}}\right) \tag{23}$$

$$\mathrm{Re}_l = \frac{G(1-\overline{x})D}{\mu_l} \tag{24}$$

$$\mathrm{Pr}_l = \left(\mu_l C_{pl} / k_l\right) \tag{25}$$

and

$$C_1 = 0.6683; C_2 = -0.2, C_3 = 1058, C_4 = 0.7$$

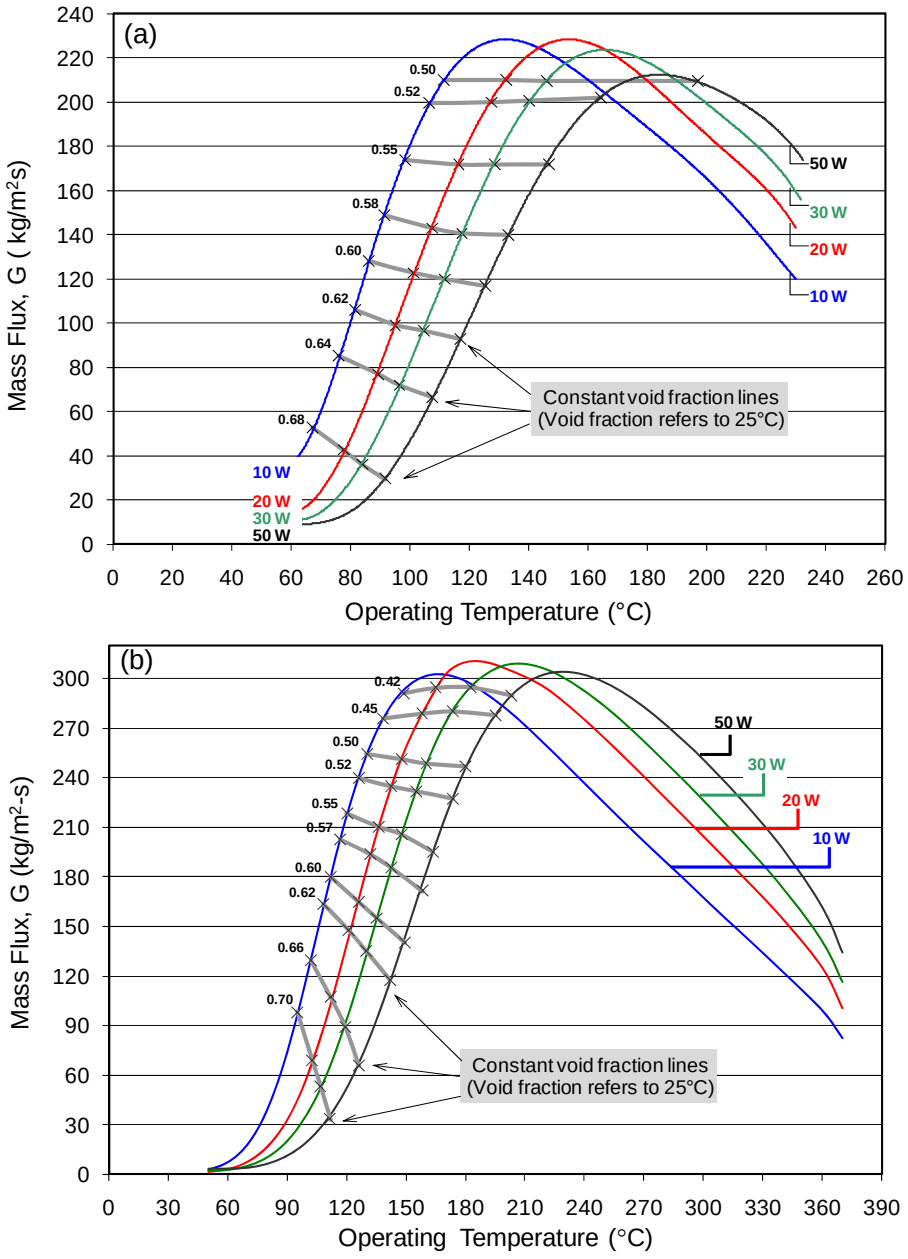

Figure 4: Operating design curve of a single loop pulsating heat pipe: (a) with ethanol as the working fluid, (b) with water as the working fluid. The geometrical parameters of the loop are L_E=L_C=75 mm, L_U=L_D= 250 mm, ID = 2.0 mm.

For calculating the heat transfer coefficient in the condenser tube section we use the Shah correlation [20] given by:

$$h_C = h_{lo}\left[(1-\overline{x})^{0.8} + \frac{3.8(\overline{x})^{0.76}(1-\overline{x})^{0.04}}{(P_{sat}/P_{crit})^{0.38}}\right] \quad (26)$$

where, h_{lo} is given by Eq. (21)

The effective thermal resistance for the single loop is given by:

$$R_{th} = \left(\frac{1}{A_E h_E} + \frac{1}{A_C h_C}\right) \quad (27)$$

where $A_E = \pi D L_E$ and $A_C = \pi D L_C$ (28)

The results of the above analysis and the effective thermal resistance for a typical case are summarized in Figure 5 (also refer Figure 1). It is clearly seen that the thermal resistance of the device decreases with increasing power input, a trend which is supported by all experimental results reported so far for on quasi-steady state PHP operational characteristics [4, 6, 9, 18, 21, 22]. Thus, simple flow boiling and condensation correlations available in the literature for mini channel geometries are effectively predicting the PHP behavior provided the correct mass flux and void distribution in the loop are known for the applied boundary conditions.

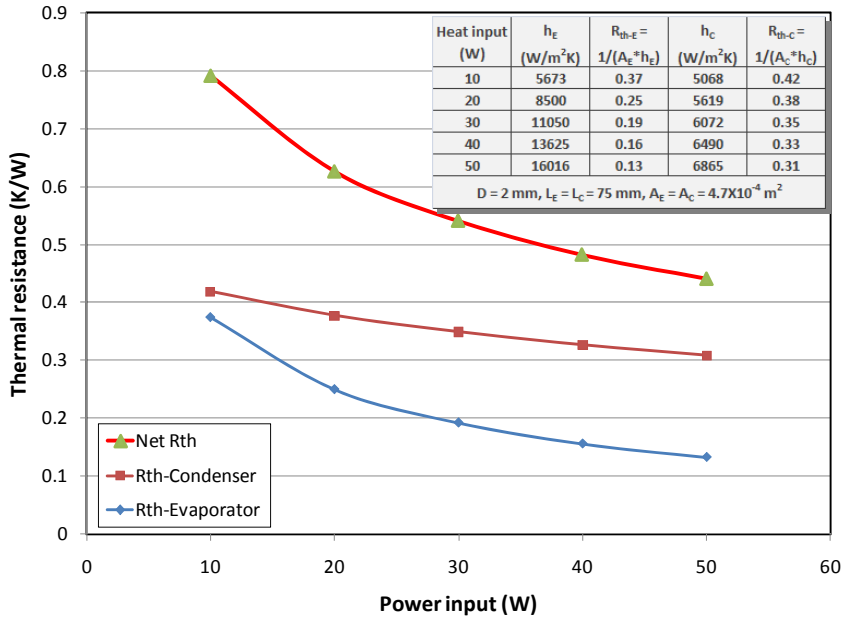

Heat input (W)	h_E (W/m²K)	$R_{th\text{-}E}$ = 1/(A_E*h_E)	h_C (W/m²K)	$R_{th\text{-}C}$ = 1/(A_C*h_C)
10	5673	0.37	5068	0.42
20	8500	0.25	5619	0.38
30	11050	0.19	6072	0.35
40	13625	0.16	6490	0.33
50	16016	0.13	6865	0.31

D = 2 mm, $L_E = L_C = 75$ mm, $A_E = A_C = 4.7X10^{-4}$ m²

Figure 5: Estimation of effective thermal resistance of a single loop pulsating heat pipe with FR = 45% and water as the working fluid with the model. As the heat power input increases the thermal resistance decreases, a typical behavior suggested by all reported PHP experiments.

5.3 Limitations of the model

Although we now have a system of closed equations to get the two-phase mass flux in the loop by the methodology described above, there are limitations about the quantitative validity and congruence of the model. With reference to real time operation of the device, these limitations can be summarized as follows:

(i) Needless to say, the abstraction of the flow as fog flow or homogeneous flow has obvious limitations. This notion only suffices as a modest beginning of the modeling exercise. A separated flow model with individual phase velocities (K>1) should be the next logical step to improve the predictions. The separated flow should consider (a) additional interfacial momentum flux dissipation due to churn/annular and annular flow in upheader and, (b) as has been reported by previous studies the effect of additional frictional resistance in the slug flow regime because of contact angle hysteresis [for example, refer 23, 24].

(ii) In real time operation of a single loop pulsating heat pipe, even if the heat flux is high enough for the fluid to circulate in the loop, the net circulation is superimposed by fluctuations of the fluid. Because of these fluctuations, the flow can never be categorized as 'fully developed laminar' or 'fully developed turbulent'. It is perpetually in the 'developing' flow mode. Thus, the effective momentum and energy transport coefficients will be substantially higher in real time as compared to the fully developed assumptions taken in the present model. If the superimposing flow fluctuations on the bulk circulating flow are incorporated, the implications on the design equation will be to considerably reduce the mass flux G at the given temperature as compared to the present predictions. This is because the dissipative friction factor will substantially increase due to the superimposed fluctuations and therefore developing nature of the flow. Nevertheless, the ensuing effective heat transfer will also increase.

(iii) The model does not take into account the additional friction or pressure drop associated with tube bends etc. This feature also tends to predict the mass flux somewhat on the higher side than what will come out in real time operation.

(iv) As will be appreciated, the solution of Eq. (19) is sensitive to the initial choice of x_i. For a small change in this value, the resulting design curve which the loop will follow will slightly get perturbed. If we constrain the operating temperature while performing the simulations then the resulting mass flux G will get perturbed. Alternately, if we constrain the mass flux G artificially then the operating temperature must get adjusted as the x_i changes to satisfy Eq. (19) along with the mass inventory constraint. In real time operation, due to continuous bubble generation and collapse processes, the downcomer experiences a fluctuating flow superimposed on the bulk circulation. Thus, the inlet vapor mass fraction fluctuates with time resulting in temperature and/or mass flux fluctuations. It is difficult to say which is the 'cause' and which the 'effect'. The simulations reported here are for 'steady' operation but real time operation is inherently 'quasi-steady'. In such nonlinear situations which are dependent on initial

conditions, the system may possess multiple steady states too. This fact has been recently reported in an experimental study [25]. In summary, a perturbation analysis needs to be incorporated to supplement this steady state results presented here.

(v) Last but not the least, the additional driving force, provided by the generation and collapse of the bubbles which becomes substantial when the number of turns becomes more than a critical number, needs to be incorporated in addition to the solitary gravity force taken in this model [1, 19]. In fact, a multi-turn device operates equally well in anti-gravity mode also. In that situation, as has been pointed out earlier in Section 2.1, $(\Delta P)_{sat}^{dyn}$ becomes the only available driving force.

6 SUMMARY AND CONCLUSIONS

The interplay of various forces governing the fundamental operating mechanism along with the design procedure of pulsating heat pipes has been described in this paper vis-à-vis other two-phase passive heat transfer systems. It is emphasized that, for the success of practical engineering design framework, the two-phase mass flux in the loop for externally applied boundary conditions needs to be determined under the constraint of conserving the total fluid mass inventory charged into the system. Following up on these lines, two-phase flow modeling of a single-loop gravity supported pulsating heat pipe is attempted considering a homogeneous fog-flow model. Two-phase flow parameters at each section of the device are estimated with this model. As in the case of two-phase thermosyphons, only the gravity head is assumed to be providing the driving potential which has to overcome the frictional resistance of the two-phase flow. It is highlighted that modeling of the dynamic pressure term due to bubble formation and collapse is the most challenging and remains to be done. The closed system of mass, momentum and energy equations leads us to estimate the net two-phase mass flux and void fraction distribution in the loop for a given initial and boundary condition. Thus, the effective thermal resistance of the device can then be determined by using correlations for convective boiling and condensation in the respective sections of the device.

It is demonstrated that vital information can indeed be extracted from such a modeling approach and this roadmap brings us one step closer to the actual real-time operation. From the standpoint of quantitatively predicting the operating parameters of the loop based on given boundary conditions, although the model presented here has many limitations, it is believed that this strategy will eventually lead to the framework for correct prediction tools for closed loop PHPs.

7 ACKNOWLEDGEMENTS

The work is partially supported by financial grants from Indian Space Research Organization (IITK/ISRO/20050083) and Board of Research for Nuclear Sciences, India (IITK/BRNS/20050292). The second author would like to thank the Department of Mechanical Engineering, IIT Kanpur for inviting him as a visiting professor during January 2008 to March 2008, during which time this manuscript was prepared. Simulations were carried out by Mr. Yati Jain, Graduate student of IIT Kanpur.

8 REFERENCES

1. Khandekar S., Thermo-Hydrodynamics of Closed Loop Pulsating Heat Pipes, Doctoral dissertation, Universitaet Stuttgart, Germany, 2004. (available at – http://elib.uni-stuttgart.de/opus/volltexte/2004/1939/).
2. Vasiliev L. L., Heat Pipes in Modern Heat Exchangers, App. Thermal Engg., Vol. 25, pp. 1-19, 2005.
3. Reay D. and Kew P., Heat Pipes, 5th edition, Butterworth-Heinemann, ISBN-10:07506675-40, 2006.
4. Zhang Y. and Faghri A., Advances and Unresolved Issues in Pulsating Heat Pipes, Heat Transfer Engg., Vol. 29, pp. 20-44, 2008.
5. Khandekar S. and Groll M., An Insight into Thermo-Hydrodynamic Coupling in Closed Loop Pulsating Heat Pipes, Int. J. of Thermal Science, Vol. 43/1, pp. 13-20, 2003.
6. Tong L. S., Wong T. N. and Ooi K., Closed-Loop Pulsating Heat Pipe, App. Thermal Engg, Vol. 21/18, pp. 1845-1862, 2001.
7. Qu W. and Ma T., Experimental Investigation on Flow and Heat Transfer of a Pulsating Heat Pipe, Proc. 12th Int. Heat Pipe Conf., pp. 226-231, Moscow, 2002.
8. Qu W., Zhou Y., Li Y. and Ma T., Experimental Study on Mini Pulsating Heat Pipes with Square and Regular Triangle Capillaries, Proc. 14th Int. Heat Pipe Conf., Florianópolis, Brazil, 2007.
9. Yang H., Khandekar S. and Groll M., Operational Limit of Closed Loop Pulsating Heat Pipes, App. Thermal Engg., Vol. 28, pp. 49-59, 2008.
10. Khandekar S., Manyam S., Groll M. and Panday M., Two-phase Flow Modeling in Closed Loop Pulsating Heat Pipes, 13th Int. Heat Pipe Conf., Shanghai, China, 2004.
11. Khandekar S. and Groll M., Insights into the Performance Modes of Closed Loop Pulsating Heat Pipes and Some Design Hints, Proc. 7th ISHMT-ASME Heat and Mass Transfer Conf., Guwahati, India, 2006.

12. Groll M. and Rösler S., Operation Principles and Performance of Heat Pipes and Closed Two-Phase Thermosyphons, J. Non-Equilibrium Thermodynamics, Vol. 17, pp. 91-151, 1992.
13. Faghri. A., Heat Pipe Science and Technology, Taylor and Francis, ISBN 1-560323833, 1995.
14. Sasin V. J., Borodkin A. A. and Feodorov V. N., Experimental Investigation and Analytical Modeling of Auto-oscillation Two-phase Loop, Proc. 9th Int. Heat Pipe Conf., Los Alamos, USA, 1995.
15. Filippeschi S., On Periodic Two-phase Thermosyphons Operating Against Gravity, Int. J. of Thermal Sciences, Vol. 45, No. 2, pp. 124-137, 2006.
16. Akachi H., Polášek F. and Štulc P., Pulsating Heat Pipes, Proc. 5th Int. Heat Pipe Symp., pp. 208-217, Melbourne, Australia, 1996.
17. Lin L., Experimental Investigation of Oscillation Heat Pipes, J. Thermophys. Heat Transfer, Vol. 15, pp. 395-400, 2001.
18. Khandekar S., Dollinger N. and Groll M., Understanding Operational Regimes of Pulsating Heat Pipes: An Experimental Study, App. Thermal Engg., Vol. 23/6, pp. 707-719, 2003.
19. Charoensawan P., Khandekar S., Groll M. and Terdtoon P., Closed Loop Pulsating Heat Pipes-Part A: Parametric Experimental Investigations, App. Thermal Engg., Vol. 23, No. 16, pp. 2009-2020, 2003.
20. Carey Van P., Liquid Vapor Phase Change Phenomena, Taylor and Francis, 2nd edition, ISBN-10: 1591690358, 2007.
21. Xu J. L., Li Y. X. and Wong T. N., High Speed Flow Visualization of a Closed Loop Pulsating Heat Pipe, Int. J. of Heat and Mass Transfer, Vol. 48, pp. 3338–3351, 2005.
22. Cai Q., Chen C. L. and Asfia J. F., Operating Characteristic Investigations in Pulsating Heat Pipe, J. of Heat Transfer, Vol. 128, No.12, pp. 1329-1334, 2006.
23. Khandekar S., Schneider M., Schaefer P., Kulenovic R. and Groll M., Thermo-fluiddynamic Study of Flat Plate Closed Loop Pulsating Heat Pipes, Microscale Thermo-physical Engineering, ISSN 1089-3954, Vol. 6/4, pp. 303-318, 2002.
24. Lips S. and Bonjour J., Oscillating Two-phase Flow in a Capillary Tube: Experiments and Modeling, Proc. 14th Int. Heat Pipe Conf., Florianópolis, Brazil, 2007.
25. Khandekar S., Gautam A. P. and Sharma P. K., Multiple Quasi-Steady States in a Closed Loop Pulsating Heat Pipe, Int. J. of Thermal Sciences, article in press, June 2008.

9 NOMENCLATURE

A : area (m^2)
C_p : specific heat (J/kg·K)
D : internal diameter (m)
G : mass flux ($kg/m^2 \cdot s$)
g : acceleration due to gravity (m/s^2)
h : heat transfer coefficient (W/m^2K)
$\hat{h}$: enthalpy (J/kg)
h_{fg} : latent heat (J/kg)
K : slip ratio
L : Length (m)
P : pressure (Pa)
ΔP : pressure drop (Pa)
Q : heat power (W)
q'' : heat flux (W/m^2)
R_{th} : thermal resistance (K/W)
T : temperature (ºC)
V : volume (m^3)
$x, \overline{x}$: two-phase vapor mass quality, average
z : linear coordinate along the tube length

Greek Symbols

$\alpha, \overline{\alpha}$: vapor void fraction, average
β : angle from horizontal (°)
ρ : density (kg/m^3)
μ : dynamic viscosity ($N \cdot s/m^2$)
ν : specific volume (m^3/kg)

Non-Dimensional Numbers

Bo : Boiling Number
C_f : Friction Factor
Co : Convection Number
Pr : Prandtl Number
Re : Reynolds Number

Abbreviations

FR : volumetric filling ratio of the working fluid (V_l/V_{tot}) at room temperature

Subscripts

Acc : fluid accumulator
avg : average
C : condenser
D : downcomer
dyn : dynamic
E : evaporator
eff : effective
f : fluid
gra : gravity
g : gas or vapor
i : inlet
ini : initial
l : liquid
lo : liquid only
m : mean
o : outlet
sat : saturation
tot : total
U : upheader
w : wall